

Multispectral 3D Surface Scanning System RoScan and its Application in Inflammation Monitoring and Quantification

Adam Chromy^{1,2}

¹Department of Control and Instrumentation, Faculty of Electrical Engineering and Communications, Brno University of Technology, Technická 3082/12, 616 00 Brno, Czech Republic

²Central European Institute of Technology, Brno University of Technology, Purkynova 656/123, 612 00 Brno, Czech Republic

Keywords: Multispectral Imaging, 3D Body Scanning, Thermal Imaging, Inflammation Monitoring, Inflammation Quantification, Treatment Evaluation.

Abstract: This paper presents experimental multispectral 3D surface scanning system RoScan, which is capable of capturing 3D models of a surface, containing a spatial representation of the object, colour of each point of the surface, its temperature and roughness. Such models are provided with accuracy up to ± 0.12 mm and thermal resolution of 0.05°C , what makes it suitable for 3D thermal body scanning in medicine. Basic principles, parameters, and functional capabilities are discussed, and developed tools for data analysis are presented. The RoScan system is suitable for early detection of inflamed regions and its objective quantification. It can be also used for evaluation of treatment suitability or for monitoring during a recovery process. To show this, the case study monitoring of inflammation related to eczema caused by an allergic reaction is presented. The inflammation development is studied using RoScan during eczema growth and after the application of two different external dermatologies – Protopic[®] 0.1% topical ointment and ointment from shea butter and coconut oil. On this particular subject, measured characteristics demonstrated a stronger effect of Protopic[®] 0.1% on eczema healing, as the evolution of inflammation in the area treated with this dermatologies started to recover earlier and culminated on the lower value of temperature gradient than the second ointment.

1 INTRODUCTION

During last years, availability of thermal imagers moved from expensive and bulky systems to affordable and practical solutions (Coffey, 2012). Development of sensors and filters reaches such advances that thermal cameras can be found already in smartphones in the price range of up to 700 EUR (Hardwicke et al., 2016). Even greater progress is evident in 3D scanning market, where a bundle of new 3D scanning devices is announced each year. Both technologies, although they are mainly applied in engineering, has capabilities, which can be useful as well in medicine.

Almost every injury, many diseases or pathological changes are characterized by increased blood flow and stronger cellular metabolic rate in the affected region, what causes the local increase of temperature (Chang et al., 2008). Such local thermal deviations can be detected and visualized by thermal cameras, working in the long-wave infrared spectrum (LWIR). Digital Medical Thermal Imaging (DMTI) is used in

many medical applications nowadays, especially in inflamed tissue analysis (Hilton-Jones, 2003; Ring and Ammer, 2012) and cancer detection (Lu and Fei, 2014).

But all current DMTI solutions suffer from a significant drawback: although the 2D thermal imaging is able to quantify the temperature of the individual pixels of the image, the DMTI is still considered a mere *qualitative tool*, enabling us to distinguish between the physiological and non-physiological states of the body but lacking the ability to *quantify* them (Vardasca and Simoes, 2013; Ju et al., 2005). This is due to three main drawbacks of DMTI: almost impossible definition of region of interest (ROI) in thermal image due to lack of recognizable clearly bounded thermal features in the image; distortions caused by transforming 3D world to 2D representation (imagine the floor plan of skyscraper – you know the coordinates inside the building but you do not know the floor); and dependence of the thermogram on the view of the camera.



Figure 1: Scanned model contains information from spatial (left), visible (middle) and LWIR spectrum (right).

The *medical quantification* itself is a general long-term problem that permeates across the entire health-care system and that is still not reliably solved.

This paper presents multispectral 3D scanning system RoScan dealing with these current drawbacks of DMTI by data fusion of 3D body scans with colour images and thermal images. This combination of sensors provides 3D surface scans covered with colour and thermal information in high resolution (Fig. 1), what enables *thermal medical quantification*. Thanks to the colour layer, the ROI can be precisely selected, the 3D model enables undistorted measurements, and thermal layer exposes non-physiological areas and provides quantifiable index reflecting the severity of a disease.

In the following text, the abilities of RoScan are outlined and the case study of monitoring inflammation related to eczema caused by an allergic reaction is presented. The inflammation development is studied using RoScan during eczema growth and after the application of two different external dermatologics.

Such studies are currently evaluated by methods that are based on different scoring systems (Necas, 2011). Individual scoring systems have different positive or negative features, but they have one thing in common - they are extremely subjective, coarse and insensitive (Sprickelman et al., 1997). As a result of this, it is impossible to quantify the immediate response of the human body immediately after drug administration. The scoring systems only reflect the long-term effect of drugs, and even if it is really significant (Lacarrubba et al., 2015).

As shown in the further text, proposed multispectral 3D scanning system RoScan enables the possibility of objective monitoring of fast temporal changes in the treated skin. Quantification of dermatitis by RoScan brings also higher sensitivity and selectivity compared to the current state of the art, as well as availability of more other quantitative parameters during the evaluation.

2 ROSCAN SCANNING SYSTEM

Because the RoScan, a multispectral scanning system using this sensor combination, brings a novel concept

in medical imaging, an extra section of this paper was devoted to introduce basic principles of this method and, in particular, to present its capabilities. From this information the reader can get an idea in which another research projects this method can be helpful.

Design of RoScan is built on the basis of Robotic 3D scanner (Chromy and Zalud, 2014a), which is composed of high-accurate 2D profile laser scanner mounted on end-point of 6-axis industrial robotic manipulator. The robot used in this device is EPSON C3, which is reaching accuracy of end-point placement $\Delta_M = \pm 0.013$ mm (Epson Robots, 2011) and the laser scanner is MicroEpsilon ScanCONTROL2750-100 with accuracy $\Delta_S = \pm 0.027$ mm (Micro-Epsilon, 2008).

Sensoric head of this robotic 3D scanning system has been extended by LWIR thermal camera Xenics GOBI1954 and colour camera ImagingSource DFK 51BG02.H (Fig. 2).

The thermal imager has resolution 384×288 pixels, pixel pitch $25 \mu\text{m}$ and spectral response of wavelength range $8 - 14 \mu\text{m}$ with the thermal resolution of 50 mK (Xenics, 2009). Colour camera ImagingSource DFK 51BG02.H has resolution 1600×1200 pixels and is supplied with $1/1.8''$ Sony CCD chip.

According to (Chromy and Zalud, 2014b), overall spatial accuracy¹ of entire RoScan scanning system is $\Delta_{Xmax} = \pm 0.12$ mm and repeatability of thermal measurements is 0.05°C .

2.1 Capturing 3D Surface Models

Capturing of 3D surface model spatial data is based on moving with the sensoric head around the scanned object by the robotic manipulator and along prede-

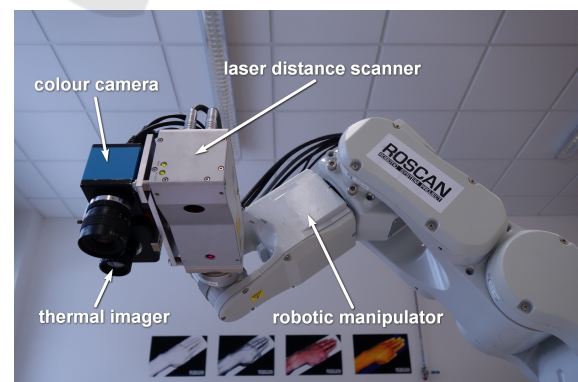


Figure 2: RoScan overview with focus on sensoric head.

¹Term accuracy in this context can be defined as maximal distance between computed (measured) position of point relative to true position of point at 99.7 % of measurements ($\pm 3\sigma$)

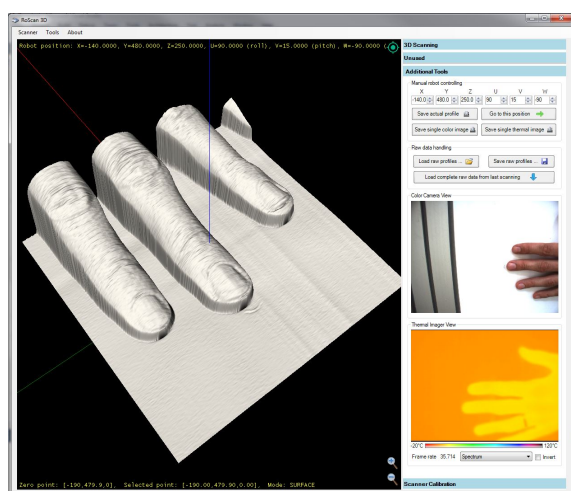


Figure 3: Software for capturing multispectral 3D surface models during process of scanning.

finer scanning trajectory. Using robotic manipulator empowers both flexibility of movement and high-accuracy of captured data, what is usually compromise between these parameters at commercially available scanners (Curless, 1999).

At each point of scanning trajectory, the laser scanner measures a distance to the scanned object along measuring line and generates output in form of 2D distance profile. Each captured profile is then further transformed to the world coordinates and linked with neighbouring data into single mesh structure. This entire process, as well as required transforming equations, is deeply described in (Chromy and Zalud, 2014a).

The software, developed for this system, allows definition of custom trajectories composed from geometric primitives using the simple scripting language. Such trajectories can be then easily launched for scanning (Fig. 3).

2.2 Mapping 2D Images onto Surface

During the scanning process, data from the colour camera and thermal imager are collected, and after building the 3D model mesh, they are projected onto the 3D surface. At this point, the ray-tracing algorithm (Suffern, 2016) is used, which examine visibility of each point of mesh from the camera. If the single point is visible from several images, the resulting temperature is given as average of values from these images. The colour in such multi-imaged points is given as linear interpolation between colours from these images, weighted by the angle relative to 3D surface normal, since the lightness of colour is influenced by the angle of light reflection.

Since the ray-tracing examination of point visibility is computationally demanding issue, the algorithm uses Octree data structure (Kunii, 2012; Burian et al., 2014), which divide the area of the 3D model into spatial cubes, in which the parts of the mesh are classified into.

This entire texture mapping process is more deeply described in (Chromy and Klima, 2017).

2.3 Mutual Calibration of Sensors

For proper mapping of thermal and colour 2D images onto 3D surface model, it is necessary to know very precisely the intrinsic parameters of camera, as well as its 6-DOF position², from which the image has been captured. This position is computed from the position of sensoric head and the position of camera relative to the sensoric head.

In order to estimate these parameters, we use the calibration method based on capturing images of calibration pattern from several angles and further comparing of evaluated extrinsic parameters with the location given by robotic manipulator. The pattern is made from PCB with the heated copper layer, which is visible on all sensors simultaneously. Calibrating cameras using this method will ensure that the images fit exactly at the right place on the 3D surface.

This method is described in (Chromy, 2017) with more details.

2.4 3D Model Analysis

An important part of RoScan scanning system is software tool for displaying and analyzing scanned images (Fig. 4). It provides functionality not only to browse through 3D models but also for various measurements of spatial properties of selected regions. It also supports export to standardized formats (e.g. PLY or PTS) for further processing of captured data in other 3D software tools.

It allows showing the scans in 4 different modes:

- **Colour** – Basic view as clinician can see the patient. This layer is mostly used for finding the visible landmarks, which are used for orientation (pigmented spots, markers drawn on skin, etc.). Such points can be highlighted to be visible also in other layers.
- **Temperature** – The layer with false colours related to the temperature of skin. The value or particular point can be examined by clicking. Slid-

²6-DOF position means 3 coordinates for camera position and 3 coordinates of rotation, defining the direction of camera view.

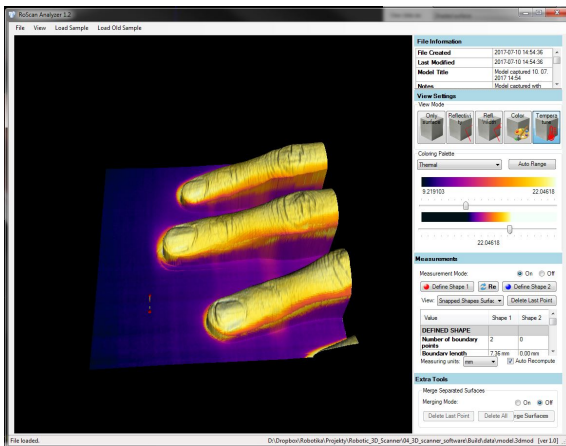


Figure 4: Software for displaying and analyzing multispectral 3D surface scans.

ers can be used to adjust colour-temperature mapping in order to see better the contrast between inflamed and healthy tissue.

- **Roughness** – Since we use the laser scanner working on triangulation principle (Smith and Zheng, 1998), besides position of reflected beam³, a divergence of reflected beam is also measured. This value corresponds to roughness of the scanned surface and can be also visualized with false colours.
- **Surface Only** – Sometimes it is important to see tiny details of the surface (like edges of the scars or boundaries of chronic wound), which are normally hidden in colors. In such cases, only the 3D surface can be displayed, without any coloring.

On each layer, the measurements tool can be activated. Following parameters can be evaluated in selected points or regions of interest (ROI):

- **Distances** [mm] – between defined points (directly, along the surface), circumferences of ROI.
- **Angles** [deg] – angle between three defined points (e.g. vertebrae positions).
- **Surface area** [mm²] – of entire model or ROI.
- **Volume** [mm³] – of entire model or ROI defined by cutting plane or deflected cutting surface.
- **Color** – of selected point or average color of ROI.
- **Roughness** – provides dimensionless index corresponding to roughness of selected point or average roughness of ROI.
- **Temperature** [°C] – of selected point or average temperature of ROI.

³At triangulation laser scanner, the position of reflected beam of detector defines the measured distance

Since the system is completely developed by author from the scratch, it can be easily adapted to any other application, within or outside of medical sector.

3 MATERIALS AND METHODS

The case study has been performed on subject suffering with the allergy on hazel allergens. The experiment began when itchy and red lesions appeared on the superior side of the left forefoot, few hours after ingestion of small amount of allergic substance. The area of the lesion had been highlighted by markers drawn on the skin and was divided into two parts, marked as *V* and *K* (Fig. 6).

During the first stage of the experiment, the subject was repeatedly scanned⁴ using RoScan during 50 minutes period. After that, Protocip[®] 0.1% topical ointment was applied to the area *K* and ointment from shea butter and coconut oil was applied to the area *V*.

During the second stage, the subject was once again repeatedly scanned using RoScan for following 31 hours. In first minutes, when a reaction to dermatologics was expected, the spacing between measurements was 2-3 minutes, then approx. 15 minutes and then about 45 minutes. Most of the measurements were taken during first 4 hours when subject was present in the laboratory. At following 27 hours, only 3 measurements were taken due to unavailability of the subject to come for measurements.

When processing the results, the areas *K* and *V* were selected on each thermal 3D scan using the colour layer of the 3D surface model, where markings drawn on the skin of the subject are visible (Fig. 5). Average temperature and selected surface area of each region were then computed⁵. The area of selected ROI serves as controlling value since it shall

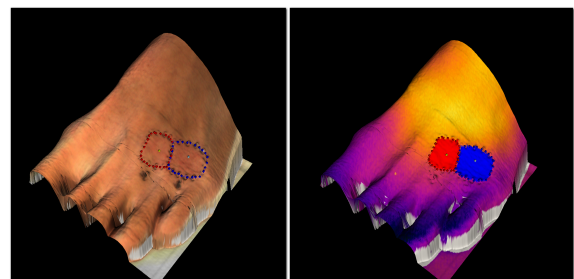


Figure 5: Selection of areas on color layer (left) and averaging of temperature on thermal layer (right).

⁴Exact time of scanning has been saved and used for further evaluation.

⁵Both values are directly provided by RoScan software tool



Figure 6: Affected area immediately after dermatologics application.



Figure 7: Affected area 31 hours after dermatologics application.

stay unchanged at all samples, even if captured from slightly different positions. The average temperature was used as the quantitative parameter.

Because surface temperature of forefoot depends also on physical activity or ambient heating, reference temperature was measured on each scan. As a reference point, the area of letter V marked on the skin was used. We are assuming, that external influences affect the entire surface equally.

For quantification of inflammation in affected area, following metric has been applied:

$$\delta_A(t) = \frac{\bar{T}_A(t) - T_R(t)}{\bar{T}_A(0) - T_R(0)} - 1 \quad (1)$$

where $\bar{T}_A(t)$ is average temperature of points belonging to the area A in time t , $T_R(t)$ is reference temperature in time t . In this context, the meaning of $\delta_A(t)$ is relative change of difference between area temperature and reference temperature, relative to the time and state when dermatologics were applied⁶. Such relative metric had been chosen due to the unequal distance of both areas from the edge of the body, what causes differences in absolute values of a temperature. This approach normalizes both values to the same scaled index and makes both areas to be comparable between each other.

Uncertainties of measurements were evaluated according to (Palencar et al., 2001) as the standard uncertainty of indirect measurement, where all 4 values influencing the results are measured with the same uncertainty of $\Delta = 0.05^\circ\text{C}$. Particular uncertainties are shown as error bars in following figures 8 - 10.

Note: Be aware, that purpose of this experiment is not to evaluate treatment efficiency of both dermatologics, but to show that RoScan is able to quantify

⁶e.g. $\delta_A(1 \text{ min}) = 10\%$ means that during first 10 minutes after application, the gradient of area temperature relative to the ref. point has grown by 10%

the inflammation and that is sufficiently sensitive for monitoring of inflammation progress. The results of this study bring information only about the reaction of this particular subject to both dermatologics and cannot be generalized to the human population.

4 EXPERIMENTAL RESULTS

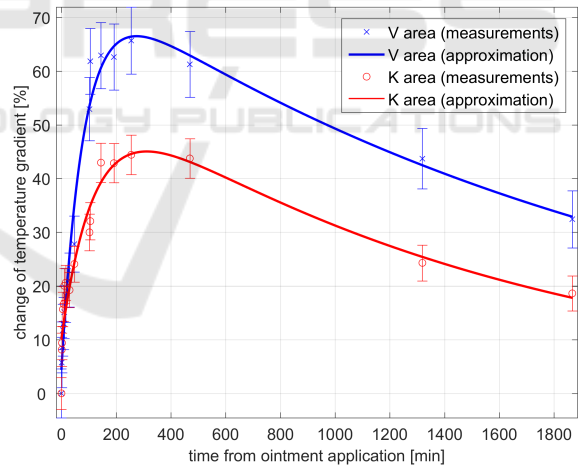


Figure 8: Development of $\delta(t)$ during 31 hours after application of ointments.

Development of $\delta_K(t)$ and $\delta_V(t)$ during 31 hours after the application of ointments is shown in Fig. 8.

The temperature gradient in the area treated by Protopic[®] 0.1% culminated at 45% gradient relatively to starting state. The area treated by ointment from shea butter and coconut oil culminated at 65%. From point of culmination, both areas are healing with a similar trend.

Both areas were similarly progressing before application of drugs, as shown in Fig. 9. Note, that

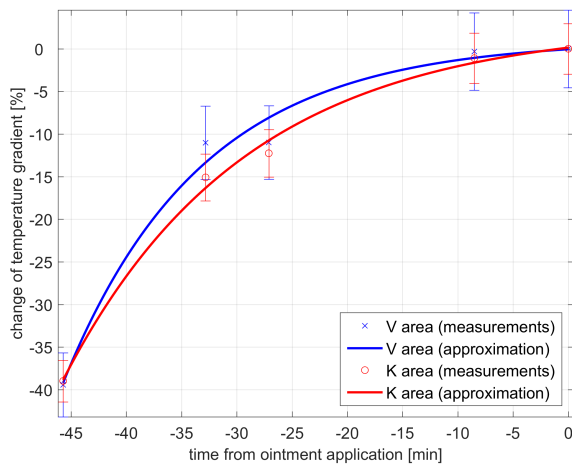


Figure 9: Development of $\delta(t)$ before application of ointments.

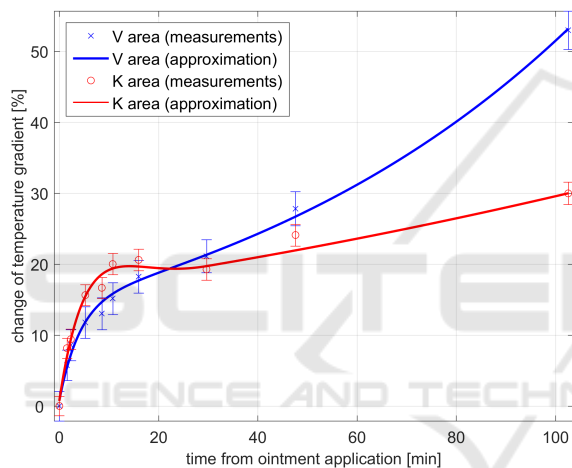


Figure 10: Detail of $\delta(t)$ characteristics in first 100 minutes after application of ointments.

there is no significant difference between the thermal progress of both areas until application of ointments. After that, the characteristics become different.

On Fig. 10, there is a detail of first 100 minutes after application, which is not visible in full scale. The temperature of area *K* is growing faster than in area *V*, but after 10 minutes stops to grow and after that, the increase during the time is significantly slower.

5 DISCUSSION

Both areas are evolving in a similar way before application of dermatologics (Fig. 9), what might rebut the assumption, that both areas are affected by differently advanced inflammation and that both areas would be then evolving differently even if not treated. For further considerations, we assume that both areas

are afflicted with inflammation of same severity, also because of the same symptoms (same redness, rash, and itching).

The active substance of Protopic[®] 0.1% is Tacrolimus (Lazarous and Kerdel, 2002), the topical calcineurin inhibitor (TCI) working by weakening the skin's defense (immune) system, thereby decreasing the allergic reaction and relieving the eczema (Baldo et al., 2009). Since atopic dermatitis is skin inflammation (Nedorost, 2012), which is partially caused by immunologic factors (Grey and Maguiness, 2016), its development should be reduced by dosing this drug.

On the contrary, the ointment from shea butter and coconut oil has no similar active substance and acts only as moisturizer (Tollefson et al., 2014), so it should serve only for prevention from cracked skin (Varothai et al., 2013).

This is in consensus with our observation from Fig. 8, where Protopic[®] 0.1% has a stronger effect on stopping the development of eczema than ointment from shea butter and coconut oil.

According to subject's feelings, 2 minutes after application of ointments, the area *K* started to be strongly burning. This feeling culminated at 7 minutes and at 12 minutes burning and itching in the area *K* fully stopped. Itching in the area *V* stays at the same level during this period. The surface of area *K* also became sticky and oozing, as shown in Fig. 11.

This report correlates with response of inflammation development in first minutes after drug application (Fig.10), where the *K* area is initially more inflamed then *V*, but then inflammation decrease speed of development more than in area *V*. The burning after an application is the well known side effect of Protopic[®] 0.1% (Lazarous and Kerdel, 2002), but its cause is not known. Anyway, it is recognizable on time evolution of 3D thermogram.

6 CONCLUSIONS

The presented paper introduced and evaluated capabilities of novel imaging technique for inflammation detection and monitoring. But the 3D + thermal + colour data fusion technology is not limited only to this domain – it can be used also in field robotics (Nejdl et al., 2015), autonomous mapping (Zalud et al., 2015) or in augmented reality (Zalud, 2006)

RoScan, the experimental equipment using this technology, is designed to producing multispectral 3D models of the body surface.

The main purpose of RoScan is being able to quantify inflammatory processes inside the human body. This inflamed region should be close to the



Figure 11: Oozing surface of area *K* after application of Protopic® 0.1%.

skin, or sufficiently "strong" to be able to influence even the skin temperature. Case study above shown, that using RoScan for quantifying inflammation is possible.

RoScan can be useful also for early detection of inflamed areas since its sensitivity is higher than commonly used methods, which are mostly based on visual observations (Lipsky et al., 2004; Krysko et al., 2008). Looking at differences between Fig. 6 and Fig. 7, it is clear, that RoScan brings more evidence-based diagnostic data, which are normally invisible. This was also shown in the presented case study.

Multispectral 3D scanning can be useful even if the symptoms are visible. The ability to preserve the exact condition of the patient's body (for comparison during the next visit at the clinician) brings the possibility to objectively evaluate the progress of a disease, even if changes are very small.

Extending 3D model with thermal information can also help in assessing if spatial changes of a body are caused by physiological (e.g. muscle growth) or non-physiological factors (e.g. edema).

On the other hand, this technology has also many limitations, when most important one is inhomogeneity of temperature distribution along body surface. The areas of higher temperature can result not only from inflammations but can be caused also by anatomical constitutions, e.g. when arteries come closer to the skin. In such areas, small inner inflammations can stay unrecognised (false negative) or the area itself can be detected as inflammation (false positive). Interpretation of 3D surface thermogram will still depend on experiences of a clinician, but it will help him to quantify the problem, what common methods can not.

ACKNOWLEDGEMENTS

This work was supported by grant No. FEKT/FIT-J-17-4745 "Intermodal 3D data registration in health-care" financed from Internal Science Fund of Brno University of Technology; by grant No. 692470, H2020, ECSEL-04-2015-Smart Health, "Advancing Smart Optical Imaging and Sensing for Health (ASTONISH)"; and by grant No. FEKT-S-17-4234 "Industry 4.0 in automation and cybernetics" financed from Internal Science Fund of Brno University of Technology.

REFERENCES

- Baldo, A., Cafiero, M., Di Caterino, P., and Di Costanzo, L. (2009). Tacrolimus ointment in the management of atopic dermatitis. *Clinical, cosmetic and investigational dermatology : CCID*, 2:1–7. PMID: 21436963 PMID: PMC3047924.
- Burian, F., Kocmanova, P., and Zalud, L. (2014). Robot mapping with range camera, CCD cameras and thermal imagers. *2014 19th International Conference on Methods and Models in Automation and Robotics (mmar)*, pages 200–205. WOS:000352788900035.
- Chang, T., Hsiao, Y., and Liao, S. (2008). Application of digital infrared thermal imaging in determining inflammatory state and follow-up effect of methylprednisolone pulse therapy in patients with graves ophthalmopathy. *Graefe's Archive for Clinical and Experimental Ophthalmology*, 246(1):45–49.
- Chromy, A. (2017). Mutual calibration of sensors for multispectral 3D scanning of surface. In *The 9th International Congress on Ultra Modern Telecommunications and Control Systems*, Munich. In Press.
- Chromy, A. and Klima, O. (2017). A 3D scan model and thermal image data fusion algorithms for 3D thermography in medicine. *Journal of Healthcare Engineering*. In press.
- Chromy, A. and Zalud, L. (2014a). Novel 3D modelling system capturing objects with Sub-Millimetre resolution. *Advances in Electrical and Electronic Engineering*, 12(5):476–487.
- Chromy, A. and Zalud, L. (2014b). Robotic 3D scanner as an alternative to standard modalities of medical imaging. *SpringerPlus*, 3(1):13.
- Coffey, V. C. (2012). Multispectral imaging moves into the mainstream. *Optics and Photonics News*, 23(4):18–24.
- Curless, B. (1999). From range scans to 3D models. *SIG-GRAPH Comput. Graph.*, 33(4):3841.
- Epson Robots (2011). Epson c3 compact 6-Axis RobotManual. [http://robots.epson.com/admin/uploads/product_catalog/files/EPSON_C3_Robot_Manual\(R7\).pdf](http://robots.epson.com/admin/uploads/product_catalog/files/EPSON_C3_Robot_Manual(R7).pdf).

- Grey, K. and Maguiness, S. (2016). Atopic dermatitis: Update for pediatricians. *Pediatric Annals*, 45(8):e280–286. PMID: 27517355.
- Hardwicke, J. T., Osmani, O., and Skillman, J. M. (2016). Detection of perforators using smartphone thermal imaging. *Plastic and Reconstructive Surgery*, 137(1):39–41. PMID: 26710006.
- Hilton-Jones, D. (2003). Diagnosis and treatment of inflammatory muscle diseases. *Journal of Neurology, Neurosurgery & Psychiatry*, 74(suppl 2):ii25–ii31. PMID: 12754326.
- Ju, X., Nebel, J., and Siebert, J. P. (2005). 3D thermography imaging standardization technique for inflammation diagnosis. In Gong, H., Cai, Y., and Chatard, J., editors, *Proceedings Volume 5640, Infrared Components and Their Applications*, page 266.
- Krysko, D. V., Vanden Berghe, T., D’Herde, K., and Vandenabeele, P. (2008). Apoptosis and necrosis: detection, discrimination and phagocytosis. *Methods (San Diego, Calif.)*, 44(3):205–221. PMID: 18314051.
- Kunii, T. L. (2012). *Frontiers in Computer Graphics: Proceedings of Computer Graphics Tokyo 84*. Springer Science & Business Media. Google-Books-ID: YYyrCAAQBAJ.
- Lacarrubba, F., Pellacani, G., Gurgone, S., Verz, A. E., and Micali, G. (2015). Advances in non-invasive techniques as aids to the diagnosis and monitoring of therapeutic response in plaque psoriasis: a review. *International Journal of Dermatology*, 54(6):626–634.
- Lazarous, M. C. and Kerdell, F. A. (2002). Topical tacrolimus protopic. *Drugs of Today (Barcelona, Spain: 1998)*, 38(1):7–15. PMID: 12532181.
- Lipsky, B. A., Berendt, A. R., Deery, H. G., Embil, J. M., Joseph, W. S., Karchmer, A. W., LeFrock, J. L., Lew, D. P., Mader, J. T., Norden, C., and Tan, J. S. (2004). Diagnosis and treatment of diabetic foot infections. *Clinical Infectious Diseases*, 39(7):885–910. PMID: 15472838.
- Lu, G. and Fei, B. (2014). Medical hyperspectral imaging: a review. *Journal of Biomedical Optics*, 19(1):010901–010901.
- Micro-Epsilon (2008). Instruction manual scanCONTROL. <http://www.micro-epsilon.cz/download/manuals/man-scanCONTROL-2700-en.pdf>.
- Necas, M. (2011). Atopicky ekzem. *Ceska dermatovenerologie*, 1(2):8–20.
- Nedorost, S. (2012). *Generalized dermatitis in clinical practice*. Springer, Dordrecht.
- Nejdl, L., Kudr, J., Ruttkay-Nedecky, B., Heger, Z., Zima, L., Zalud, L., Krizkova, S., Adam, V., Vaculovicova, M., and Kizek, R. (2015). Remote-Controlled robotic platform for electrochemical determination of water contaminated by heavy metal ions. *International Journal of Electrochemical Science*, 10(4):3635–3643. WOS:000352222500069.
- Palencar, R., Vdolecek, F., and Halaj, M. (2001). Nejistoty v mereni ii: nejistoty primych mereni. *Automa*, 2001(10):55–56.
- Ring, E. F. J. and Ammer, K. (2012). Infrared thermal imaging in medicine. *Physiological Measurement*, 33(3):R33.
- Smith, K. B. and Zheng, Y. F. (1998). Accuracy analysis of point laser triangulation probes using simulation. *Journal of Manufacturing Science and Engineering*, 120(4):736–745.
- Sprickelman, A. B., Tupker, R. A., Burgerhof, H., Schouten, J. P., Brand, P. L., Heymans, H. S., and van Aalderen, W. M. (1997). Severity scoring of atopic dermatitis: a comparison of three scoring systems. *Allergy*, 52(9):944–949. PMID: 9298180.
- Suffern, K. (2016). *Ray Tracing from the Ground Up*. CRC Press. Google-Books-ID: .RDYCWAAQBAJ.
- Tollefson, M. M., Bruckner, A. L., and Section On Dermatology (2014). Atopic dermatitis: skin-directed management. *Pediatrics*, 134(6):e1735–1744. PMID: 25422009.
- Vardasca, R. and Simoes, R. (2013). Current issues in medical thermography. In *Topics in Medical Image Processing and Computational Vision*, Lecture Notes in Computational Vision and Biomechanics, pages 223–237. Springer, Dordrecht. DOI: 10.1007/978-94-007-0726-9_12.
- Varothai, S., Nitayavardhana, S., and Kulthanan, K. (2013). Moisturizers for patients with atopic dermatitis. *Asian Pacific Journal of Allergy and Immunology*, 31(2):91–98. PMID: 23859407.
- Xenics (2009). Xenics GOBI 1954 reference manual.
- Zalud, L. (2006). ARGOS - system for heterogeneous mobile robot teleoperation. In *2006 IEEE/RSJ International Conference on Intelligent Robots and Systems, IROS 2006*, pages 211–216, Beijing; China.
- Zalud, L., Kocmanova, P., Burian, F., Jilek, T., Kalvoda, P., and Kopecny, L. (2015). Calibration and evaluation of parameters in a 3D proximity rotating scanner. *Elektronika ir Elektrotechnika*, 21(1):3–12.